THE JOURNAL OF PHYSICAL CHEMISTRY B

Article

pubs.acs.org/JPCB

A Computational Study of Anion-Modulated Cation−π Interactions

Jorge A. Carrazana-García,[†] Jesús Rodríguez-Otero,[‡] and Enrique M. Cabaleiro-Lago*[,†]

[†]Departamento de Química Física, Facultade de Química, Universidade de Santiago de Compostela, Campus de Lugo, Avenida Alfonso X El Sabio s/n 27002 Lugo, Spain

[‡]Departamento de Química Física, Facultade de Ciencias, Universidade de Santiago de Compostela, Avenida das Ciencias s/n, 15782 Santiago de Compostela, Spain

Supporting Information

ABSTRACT: The interaction of anions with cation−π complexes formed by the guanidinium cation and benzene was thoroughly studied by means of computational methods. Potential energy surface scans were performed in order to evaluate the effect of the anion coming closer to the cation−π pair. Several structures of guanidinium−benzene complexes and anion approaching directions were examined. Supermolecule calculations were performed on ternary complexes formed by guanidinium, benzene, and one anion and the interaction energy was decomposed into its different two- and three-body contributions. The interaction energies were further dissected into their electrostatic, exchange, repulsion, polarization and dispersion contributions by means of local molecular orbital energy decomposition analysis. The results confirm that, besides the electrostatic cation−anion attraction, the effect of the anion over the cation−π interaction is mainly due to polarization and can be rationalized following the changes in the anion−π and the nonadditive (three-body) terms of the interaction. When the cation and the anion are on the same side of the π system, the three-body interaction is anticooperative, but when the anion and the cation are on opposite sides of the π system, the three-body interaction is cooperative. As far as we know, this is the first study where this kind of analysis is carried out with a structured cation as guanidinium with a significant biological interest.

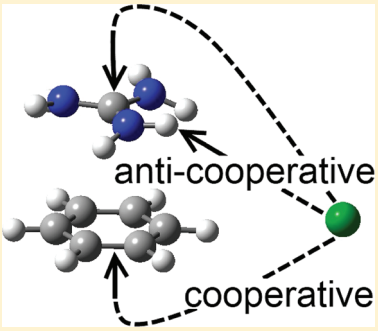

1. INTRODUCTION

Among the most important steps toward the comprehension of important biological systems and processes, an outstanding place is occupied by the progressive understanding of noncovalent interactions.[1−4] Among these forces, an important role is played by interactions between charged species and π systems, and their contribution to molecular recognition, protein structure, enzyme−substrate interaction, and many other aspects of biochemistry have been widely documented.[4−7] At the same time, these interactions have a remarkable presence in the modern and promising fields of supramolecular chemistry and technology.[8,9]

A great number of experimental and theoretical investigations have been devoted to the cation−π interactions, highlighting their relevance in a wide variety of processes. These studies have come to an agreement in that the nature of cation−π interaction is mainly electrostatic[5,6,10−18] but with an important contribution of inductive forces[19−21] especially when extended high-polarizable π systems participate.[22]

The interaction of anions and aromatic systems in the so-called anion−π interaction has only recently aroused the interest of researchers after several studies emerged demonstrating the possibility of favorable interactions between anions and aromatic systems substituted with electron-withdrawing groups.[23−26] The interpretation of anion−π interactions is more difficult, and the studies in this area are more recent and less numerous,[23,25,27−30] but there seems to be a validated understanding about their similar electrostatic plus polarization nature and that the contribution of dispersion forces is crucial in their complete description.[29,30]

Nevertheless, the studies of these interactions have been focused almost exclusively in binary (cation−π or anion−π) complexes separately. In real systems, however, the environment surrounding an ion−π complex can modulate the strength and characteristics of the interaction, as already shown in several studies about the influence of a small number of water molecules over the cation−π interaction.[31−38] In a similar way, the presence of adjacent counterions asserts the problem of the mutual influence in the combined cation−π−anion association,[14,15,39−43] a topic that had been mostly addresses at a semiempirical level.[44,45]

The pioneering work of Kim et al.[43] in the ab initio study of these ternary systems pointed out the central importance of nonadditive contributions, also highlighted by Deyá and coworkers after their quantum mechanical study of multiple complexes[46] that include cation−π and anion−π fragments. Kim's work also discusses the significance of the charge transfer as the origin of the weakening in the cation−π interaction in the anion−cation−π arrangement. These authors have found that when the ternary complex presents a linear arrangement, with the cation and anion occupying opposite sides of a benzene ring, the polarizing effect of the cation over the π cloud

Received: March 8, 2012
Revised: May 3, 2012
Published: May 3, 2012

   dx.doi.org/10.1021/jp302271y | J. Phys. Chem. B 2012, 116, 5860−5871

significantly increases the binding of the anion to the complex.[43] However, in Kim et al.'s work,[43] only simple alkaline cations and halogen anions occupying opposite sides of the aromatic ring were considered.

In the present work, the modulating effect of an anion over the cation−π interaction is studied theoretically using detailed ab initio calculations on some model complexes in which the total interaction and also the two-body and three-body (nonadditivity) terms are evaluated in a variety of configurations of the complexes not restricted to a linear arrangement. As the π system, the benzene ring present, for example, in phenylalanine has been employed. Among the different cations that can be involved in a cation−π interaction, the guanidinium cation is of special interest as it constitutes the cationic extreme of the side chain of arginine. The guanidinium cation exhibits several remarkable characteristics, being a planar cation with a tendency to form stacked structures, even between solvated guanidinium units.[47−52] It is also widely used as a denaturant and as a basic unit for constructing anion selective receptors or ionic liquids.[53,54] The anions employed in the present study (chloride, bromide, and nitrate) also have a prominent role in many biological systems. These choices give the methods, analysis, and conclusions of this study a potential interest in diverse fields of biological science as well as in the supramolecular design dealing with oligo- and polypeptides, enzymes, ionic channels, and other concurrent areas where amino-acids with cationic and/or aromatic residues interact with anions forming ternary cation−π−anion complexes.

2. COMPUTATIONAL DETAILS

The potential energy surface of ternary cation−π−anion complexes was explored by performing geometry optimizations using different starting geometries. The stationary points found were characterized as minima by frequency calculations. Both the M062X/6-31+G* and the MP2/6-31+G* levels of calculation were used in these calculations. For the minima, the interaction energies were calculated employing the supermolecule method[55] with different levels of theory, including CCSD(T)/aug-cc-pVDZ, and decomposed according to their physical origin as well as their pair contributions (see below). In all calculations, the basis set superposition error (BSSE) was corrected by employing the counterpoise method.[55,56] Optimizations, frequency calculations and counterpoise calculations were carried out with the Gaussian 09 suite of programs.[57]

In order to gain more understanding about how the presence of the anion affects the cation−π interaction, the potential energy surface of the complexes was explored by performing a series of calculations keeping the geometry of the cation−π unit fixed, whereas the anion is located at different distances from the cation following several approaching directions. The use of a polyatomic cation as guanidinium implies a variety of more complex situations than when a monatomic cation is used in the study of cation−π complexes. In order to systematize the study focusing the attention on a small number of configurations, some simplifications have been applied. First, benzene−guanidinium (BG) complexes were optimized at the MP2/6-31+G* and M062X/6-31+G* levels looking for three basic arrangements: perpendicular, parallel, and parallel displaced (**T**, **P** and **D**, respectively) as shown in Figure 1. Second, keeping the geometry of a particular BG complex frozen, the influence of the anion (X) was explored by approaching the anion following the three directions shown in Figure 1, giving a total of nine scans for each anion.

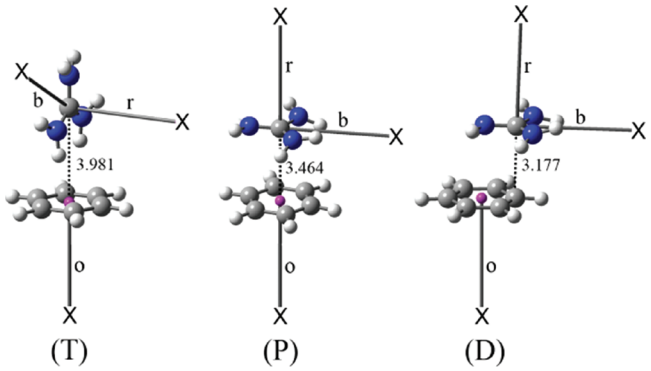

Figure 1. Geometries of the binary cation−π complexes. Benzene−guanidinium distances shown (dot lines) are in Å and correspond to BG complexes optimized at the MP2/6-31+G(d) level. The directions employed for approaching the anion X to the BG complexes are labeled as follows: b = bisector of G; r = right angle to the plane of G; o = with X and G in the opposite sides of B.

The interaction energy was then obtained at each point of the scans at the MP2/aug-cc-pVDZ and M062X/6-31+G* levels of calculation and decomposed into its pair contributions. Both levels of calculation reproduce quite well the energy values calculated at the CCSD(T)/aug-cc-pVDZ level (see below and Supporting Information). A more exhaustive study was performed for complexes containing chloride anion at the MP2/aug-cc-pVDZ level of calculation, while M062X/6-31+G* was mainly used in the explorations with other anions. The following set of seven energies has been obtained for a given geometry of the cation−π−anion ternary complex employing the whole basis set of the complex to avoid BSSE: the energies of the complex (E_T), the three pair combinations (E_{BG}, E_{BX}, E_{GX}), and the three independent fragments (E_B, E_G, E_X). Combining these seven energies allows the calculation of the BSSE-corrected interactions: $E_{\pi-G-X}$ (total), $E_{\pi-G}$ (cation−π), $E_{\pi-X}$ (anion−π), E_{G-X} (cation−anion) and the 2 + 1 interactions, for example, $E_{\pi G-X}$ is the (cation+π)−anion interaction. By means of the usual equations applicable in many-body analysis,[55,58,59] the three-body interaction (E_{thr}) can be calculated as well. E_{thr}, also called cooperativity or anticooperativity,[46,60] depending on its sign, gives valuable information regarding the interplay between all the noncovalent interactions present in the ternary complexes and expresses the nonadditive term of the interactions in these three-body systems. The definition:

$$E_{\pi-E-X} = E_{G-X} + E_{\pi-G} + E_{\pi-X} + E_{thr} \quad (1)$$

applied to the present study emphasizes the fact that the total interaction observed in these scans is determined by the strong cation−anion interaction plus a constant cation−π interaction (the geometry of the BG interaction is kept fixed) and modified by the weak anion−π and three-body interactions.

Finally, the different contributions to the interaction energies were obtained by using the local molecular orbital energy decomposition analysis (LMO-EDA) method developed by Su and Li[61] as implemented in GAMESS.[62,63] This approach is an extension of the methods developed by Kitaura and Morokuma,[64] Ziegler and Rauk,[65] and Hayes and Stone.[66] The interaction energy has been decomposed into its electrostatic, exchange, repulsion, and polarization contribu-

dx.doi.org/10.1021/jp302271y | J. Phys. Chem. B 2012, 116, 5860−5871

tions, using the Hartree−Fock or density functional theory (DFT) wave functions for every ternary complex and all possible pairs in each point of the scans. Additionally, the dispersion contribution is evaluated as the difference between the total interaction energy, calculated at the level of theory used, and the sum of all the previous contributions obtained at the HF/DFT level[61] (although this corresponds more precisely to the contribution of the correlation energy to the interaction, at least with MP2). The counterpoise method proposed by Boys and Bernardi[56] for correcting the BSSE is implemented in LMO-EDA so that the monomers use the supermolecule basis set.

3. RESULTS AND DISCUSSION

First, results obtained from optimization of the ternary complexes will be briefly discussed, devoting the rest of the exposition to analyze the results of the scans performed by varying the distance between the anion and the cation−π complexes. Most results will be presented for chloride complexes, dedicating the last section to discuss the differences found when other anions such as bromide or nitrate are considered.

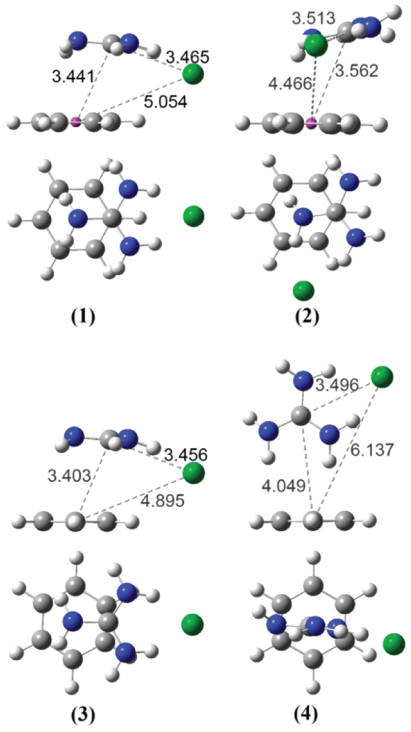

Figure 2. Side and top views of the four minima of the benzene−guanidinium−chloride complex found at the MP2/6-31+G(d) level of calculation. The centroid of the benzene ring and the central carbon atom of the guanidinium cation are used as reference points for defining the G−X, B−G, and B−X distances (in Å).

3.1. Ternary Cation−π−Chloride Complexes. Figure 2 shows the four minima found for the benzene−guanidinium−chloride system (BGX with X = Cl^-) as well as the B−G, B−X, and G−X distances, using the centroid of the benzene ring and the central carbon atom of guanidinium as reference points.

The total interaction energy and its decomposition into two- and three-body interactions, calculated at different levels of theory for the four minima of the benzene−guanidinium−chloride ternary complexes shown in Figure 2 are presented in Table 1. These configurations, all with the anion and cation in the same side of the π-system, were found using a variety of starting geometries. No minima were found with the ions located on opposite sides of the benzene plane, indicating that in the cation−π−anion complexes, the ion pairing has a dominant stabilizing effect over the total interaction. It can be observed that the most stable structures present the guanidinium cation parallel to the benzene ring, whereas in minimum **4** guanidinium is located perpendicularly, being the least stable minimum. These results are in contrast with those obtained for isolated guanidinium−benzene complexes, where the structure with guanidinium perpendicular to benzene is clearly the most stable one.[33,36] Of course the differences should be a consequence of the presence of the anion modulating the interaction and also establishing favorable interactions with the benzene ring.

Table 1. Total and Pair Interactions in the Four Minima Found in the Benzene−Guanidinium−Chloride System Obtained Using Different Levels of Calculation[a]

	total	π−G	π−X	G−X	thr
		1			
M062X/6-31+G*	−125.49	−11.54	−5.15	−114.54	5.74
M062X/aVDZ	−127.07	−11.45	−5.47	−116.48	6.33
MP2/6-31+G*	−117.50	−8.48	−4.52	−110.15	5.65
MP2/aVDZ	−124.60	−10.64	−5.44	−114.78	6.26
CCSD(T)/aVDZ	−122.49	−9.57	−5.29	−114.05	6.43
		2			
M062X/6-31+G*	−123.83	−11.53	−3.80	−113.98	5.48
M062X/aVDZ	−125.71	−11.60	−4.32	−116.04	6.25
MP2/6-31+G*	−115.51	−9.29	−2.10	−109.33	5.21
MP2/aVDZ	−123.04	−11.46	−3.54	−114.06	6.01
CCSD(T)/aVDZ	−120.72	−10.28	−3.30	−113.31	6.17
		3			
M062X/6-31+G*	−126.16	−11.33	−5.95	−114.59	5.71
M062X/aVDZ	−127.71	−11.19	−6.34	−116.48	6.31
MP2/6-31+G*	−117.65	−8.46	−4.45	−110.23	5.50
MP2/aVDZ	−124.82	−10.61	−5.48	−114.87	6.13
CCSD(T)/aVDZ	−122.67	−9.53	−5.31	−114.14	6.31
		4			
M062X/6-31+G*	−120.98	−13.62	0.77	−113.50	5.37
M062X/aVDZ	−123.39	−14.11	0.64	−115.86	5.95
MP2/6-31+G*	−115.62	−12.45	0.71	−109.19	5.32
MP2/aVDZ	−122.19	−14.41	0.45	−114.11	5.87
CCSD(T)/aVDZ	−120.35	−13.34	0.44	−113.31	5.86

[a]All values are in kcal/mol, and aVDZ stands for aug-cc-pVDZ.

Considering the pair contributions as listed in Table 1, it can be observed that the total interaction is clearly dominated, as could be anticipated, by the strong cation−anion attraction, but at the same time other pair interactions (except $E_{\pi-X}$ for the minimum **4**) present values that are non-negligible. As expected, the cation−π ($E_{\pi-G}$) interaction is moderately attractive in the four systems, with **4** being the minimum that shows the strongest cation−π interaction due to the direct facing of the hydrogen atoms of guanidinium with the benzene's π cloud, as already shown in previous work in binary systems.[33,36] In addition, the anion−π ($E_{\pi-X}$) interaction is attractive in **1**, **2**, and **3** minima, where the benzene−chloride distance is between 4.5 Å and 5.1 Å, but it is almost zero in minimum **4**, where the Cl^- is at 6.1 Å from the benzene

dx.doi.org/10.1021/jp302271y | J. Phys. Chem. B 2012, 116, 5860−5871

centroid. In all these ternary complexes, the nonadditive term is anticooperative ($E_{thr} > 0$), and the cation−anion interaction has similar values, with the sum of $E_{\pi-X}$ + E_{thr} being what determines the relative magnitudes of the total interaction.

Regarding the levels of theory reported in Table 1, all perform similarly, with MP2/aug-cc-pVDZ and M062X/6-31+G* reproducing the values of CCSD(T)/aug-cc-pVDZ somewhat better than the other levels. On the other hand, the MP2/6-31+G* level, except for the E_{thr} interaction, systematically gives energies that are less negative, behaving a little worse than the other levels of calculation analyzed.

The total interaction energies of the BGX minima were decomposed using the LMO-EDA method,[61] the results being presented in Table 2. Considering that dispersion contribution

Table 2. LMO-EDA Analysis of the Total Interaction Energy of the Four Benzene−Guanidinium−Chloride Minima Found at the CCSD(T)/aug-cc-pVDZ[a]

ternary complex	1	2	3	4
elec.	−134.00	−130.70	−133.97	−129.68
exch.	−67.46	−68.45	−67.47	−60.01
rep.	120.34	121.26	120.13	109.97
pol.	−28.05	−29.11	−27.88	−29.36
disp.	−13.32	−13.72	−13.48	−11.27
$E_{\pi-G-X}$	−122.49	−120.72	−122.67	−120.35

[a]All values are in kcal/mol.

is not properly defined with this method, a comparison was done with values obtained applying a more rigorous approach as SAPT(DFT)[67,68] as implemented in Molpro.[69] Details of these calculation and the values obtained for the different molecular pairs are included as Supporting Information. Although differences arise, the values and trends observed are pretty similar between LMO-EDA and SAPT(DFT), so it can be expected that the values obtained from LMO-EDA calculations provide a reasonable description of the different contributions to the interaction. Regarding the values in Table 2, all observed trends are very similar in the four cases, showing electrostatic and repulsion as the major contributions (of course, with opposite signs), with the rest of the contributions all being moderately attractive and having the same order of importance: exchange > polarization > dispersion. The values observed in the contributions to the total interaction of these structures are easily related with the respective geometries. Minimum **4**, with the largest B−G and B−X distances, presents the less attractive exchange and dispersion contributions as well as the smallest repulsion energy. The G−X distance is similar in this complex and in minimum **2**, and both present comparable values of the electrostatic contribution to their total interaction. The same is observed when the electrostatic contributions for minima **1** and **3**, with almost identical G−X distances, are compared.

3.2. Approaching an Anion to Cation−π Complexes.

As stated in the Computational Details section, three configurations of the benzene−guanidinium complexes were used for exploring the influence of an anion on the cation−π interaction (see Figure 1): **P** (benzene parallel to guanidinium), **D** (parallel displaced), and **T** (guanidinium cation perpendicular to the benzene plane). These are idealized structures similar to the main benzene−guanidinium motifs found in the ternary complexes analyzed and in benzene−guanidinium dimers,[33,36] but some simplifications were applied. The three binary complexes were optimized forcing C3 symmetry in **P**, C2 symmetry in **T**, and the position of the guanidinium cation parallel over one C−H bond of benzene in **D**.

The results obtained at the MP2/aug-cc-pVDZ//MP2/6-31+G* level are shown in Table 3. Comparing the three

Table 3. Interaction Energy and Its LMO-EDA Decomposition at the MP2/aug-cc-pVDZ//MP2/6-31+G* Level for the Three Geometries of the Benzene−Guanidinium Complexes Considered in This Study[a]

binary complex	P	D	T
elec.	−7.12	−9.43	−11.76
exch.	−8.50	−13.13	−4.77
rep.	14.74	23.01	27.14
pol.	−2.99	−4.55	−9.03
disp.	−5.33	−6.66	−6.15
$E_{\pi-G}$	−9.19	−10.76	−14.57

[a]See Figure 1.

configurations of the BG complex studied here, the strongest interaction, as indicated in the literature,[33,36] is found in **T**, where the hydrogen atoms of guanidinium, which concentrate most of the positive charge of the cation, are pointing directly toward the π cloud of benzene. This is the same situation already analyzed in the ternary complex **4**. On the other extreme is **P**, where the hydrogen atoms of guanidinium are all on top of the peripheral zone of benzene. Displacing the guanidinium above one C−H bond of the benzene in **D** locates some of the guanidinium hydrogen atoms directly over the π cloud of benzene, favoring the interaction. This complex shows an intermediate value of the interaction energy, in comparison with **T** and **P**.

As expected, the largest contribution to the interaction energy comes from electrostatic plus exchange, with polarization and dispersion contributing significantly, in agreement with previous results.[36] Also, dispersion contribution is more important in parallel structures than in the **T** one. Because of the same geometrical considerations, a sequence identical to that for the total interaction is observed in the electrostatic, polarization, and repulsion components.

Keeping the benzene−guanidinium complex frozen at these optimized structures, the effect of bringing an anion near a cation−π complex was systematically studied approaching the anion (X) to the three benzene−guanidinium complexes, following in each case three directions, as shown in Figure 1. At every BG−X distance, the total interaction was separated in its pair contributions, and additionally E_{thr} was calculated.

The complete set of total interaction energy values (calculated at the MP2/aug-cc-pVDZ level) and the distances corresponding to the minima in the nine BGX scans (with X = Cl^-) studied is presented in Table 4. It is observed that the geometry of the BG complex has a minor influence in the position of the minima of these scans; the BG−X distances in Table 4 are almost the same for each X-approaching direction, and the values of $E_{\pi-G-X}$ in the minimum are also clearly grouped according to **b**, **r**, or **o** scans (see Figure 1). The most intense $E_{\pi-G-X}$ interaction corresponds to the direct interaction of chloride anion with the hydrogen atoms of guanidinium (scans **b**), the intermediate $E_{\pi-G-X}$ values are for the interaction of Cl^- with the center of the guanidinium cation (scans **r**), and the smallest are for the structures with the anion facing the π cloud of benzene (scans **o**).

dx.doi.org/10.1021/jp302271y | J. Phys. Chem. B 2012, 116, 5860−5871

Table 4. Interaction Energy ($E_{\pi-G-X}$ in kcal/mol) and Distances in Å for the Minima in the Nine BGX Scans Studied, As Obtained at the MP2/aug-cc-pVDZ Level[a]

	P-b	D-b	T-b
$E_{\pi-G-X}$	−110.60	−113.05	−112.99
r_{G-X}	3.48	3.47	3.48
	P-r	**D-r**	**T-r**
$E_{\pi-G-X}$	−87.18	−89.18	−95.56
r_{G-X}	2.99	3.00	2.98
	P-o	**D-o**	**T-o**
$E_{\pi-G-X}$	−61.48	−64.50	−69.12
r_{G-X}	6.62	6.48	7.10
r_{B-X}	*3.16*	*3.15*	*3.12*

[a]The geometry of the benzene−guanidinium dimer is fixed to the values of MP2/6-31+G* optimized geometry.

3.2.1. Pair Interactions. The results obtained at the MP2/aug-cc-pVDZ level of calculation for the **P-b**, **P-r**, and **P-o** scans are shown in Figure 3 (and in Figures S1 and S2 of the Supporting Information for the **T** and **D** scans), where **b**, **r**, and **o** indicate the approaching direction of X to the BG complex, as shown in Figure 1. The interaction for systems containing fragments with opposite charge are grouped in Figure 3I,III,V, and the rest are grouped in Figure 3II,IV,VI. It can be observed the great magnitude of contributions dominated by the electrostatic interaction that propagates to very large distances. When chloride is separated by a distance as large as 12 Å from the cation−π complex (in the **P-o** scan, it means r_{G-X} = 15.46 Å because, in the complex **P**, the distance r_{B-G} is 3.46 Å, as can be seen in Figure 1), $E_{\pi G-X}$, E_{G-X}, and the total $E_{\pi-G-X}$ interactions are all still between −35.5 and −28.1 kcal/mol. These values are still far from the asymptotic ones ($E_{\pi-G}$ for $E_{\pi-G-X}$ and $E_{\pi G-X}$, and zero for E_{G-X}) that will only be achieved at very large BG−X distances. The contributions plotted in Figure 3I,III present the minimum at the same guanidinium−chloride distance (3.48 Å in **P-b** and 2.99 Å in **P-r**), indicating that in the **b** and **r** scans, the large electrostatic forces between opposite charges have a clear influence on the equilibrium distance where the interaction is more favorable ($E_{\pi-G-X}$ more negative). All the scans in which the anion approaches the cation by the same side of the π-system present the same results.

On the other hand, in the scans by the **o** direction, the opposite charges are separated by larger distances, and when X reaches the shortest distance explored, E_{G-X} has not achieved its minimum, as can be seen in its monotone behavior in Figure 3V, but the total interaction shows a well-defined minimum at r_{B-X} = 3.16 Å (r_{G-X} = 6.62 Å). This result reveals that when the cation and the anion are in opposite sides of the π-system, the distance of the more favorable configuration is not defined directly by the cation−anion attraction but by a combination of the π−X repulsion and three-body contributions (in any particular scan, π−G interaction is constant and has no effect on the position of the minima).

It can be observed in plots I, III and V of Figure 3 (and in Figures S1 and S2) that the difference between $E_{\pi-G-X}$ and $E_{\pi G-X}$ is always constant. This is true for all the systems studied in this work because, for every particular scan, the geometry of the benzene−guanidinium complex was kept fixed, and it can be demonstrated that

$$\begin{aligned} E_{\pi-G-X} - E_{\pi G-X} &= (E_{BGX} - E_B - E_G - E_X) \\ &\quad - (E_{BGX} - E_{BG} - E_X) \\ &= (E_{BG} - E_B - E_G) \\ &= E_{\pi-G} \end{aligned} \tag{2}$$

Following the same method, we now relate two other strong interactions:

$$\begin{aligned} E_{\pi-G-X} - E_{G-X} &= (E_T - E_{GX} - E_B) \\ &= E_{\pi-G} + E_{\pi-X} + E_{thr} \end{aligned} \tag{3}$$

This means that the difference between $E_{\pi-G-X}$ and E_{G-X} is constant when both E_{thr} and $E_{\pi-X}$ go to zero or when these last two interactions have opposite sign and similar absolute values. The latter condition is the case of the **P-b** scan presented in Figure 3I, where $E_{\pi-G-X}$ and E_{G-X} are separated by a constant value once $E_{\pi-X}$ (attractive) and E_{thr} (repulsive) cancel each other at about 5.5 Å and beyond. This is the rule in all the **P-b**, **T-r**, and **D-b** scans. On the other hand, in the **P-r** scan, the three-body and the anion−π interactions are both repulsive (Figure 3IV). The same can be seen for **T-b** and **D-r** scans. In these systems, the curves of $E_{\pi-G-X}$ and E_{G-X} do not reach the constant separation (equal to the value of $E_{\pi-G}$) up to the longest BG−X distance explored in this study (12 Å). In the scans where X approaches the BG complexes by the **o** direction (**P-o**, **T-o**, and **D-o**), $E_{\pi-X}$ and E_{thr} again have opposite signs. In these cases, $E_{\pi-X}$ is repulsive and E_{thr} attractive, but their magnitudes are never comparable being that the cooperativity is always more intense than the anion−π repulsion. In neither of these cases does the term ($E_{\pi-X}$ + E_{thr}) disappear in the interval of BG−X distances up to 12 Å.

Independently of the BG geometry and the X approaching direction, at BG−X distances much longer than 12 Å, the difference between the total and the cation−anion interactions will be constant and equal to the cation−π interaction, because of the eventual disappearance of the $E_{\pi-X}$ and E_{thr} contributions.

The analysis of the pair interactions shows that when the opposite charges are on the same side of the π-system allowing the ion pairing, the strong interactions determined by the electrostatic forces control the most stable ternary complex configuration, but the relationships between these intense interactions depend on the weak interactions $E_{\pi-X}$ and E_{thr}. When the cation and anion are on opposite sides of the π system, the importance of the weak interactions is even larger. In any case, the modulating effect of the anion over the cation−π interaction can be ascertained by $E_{\pi-X}$ and E_{thr}. Because $E_{\pi-G-X}$ is more than 1 order of magnitude larger than $E_{\pi-X}$ and E_{thr}, the study of the influence of an anion over the cation−π interaction cannot be made in terms of the total interaction; an analysis of this interaction into its pair components is necessary.

Figure 4I shows the results obtained for the anion−π interaction along the different BGX scans with X = Cl^-. As stated above, $E_{\pi-X}$ is attractive in the **P-b** scan as well as in the **D-b** and **T-r** scans, where the X-approaching direction is parallel to the benzene plane, allowing an interaction between the anion and one of the hydrogen atoms of benzene. In **P-b** and **T-r**, such interaction is reflected by a minimum in the anion−π interaction profile at an r_{G-X} distance of about 4 Å. This minimum is deeper in **P-b** because the anion passes closer

dx.doi.org/10.1021/jp302271y | J. Phys. Chem. B 2012, 116, 5860−5871

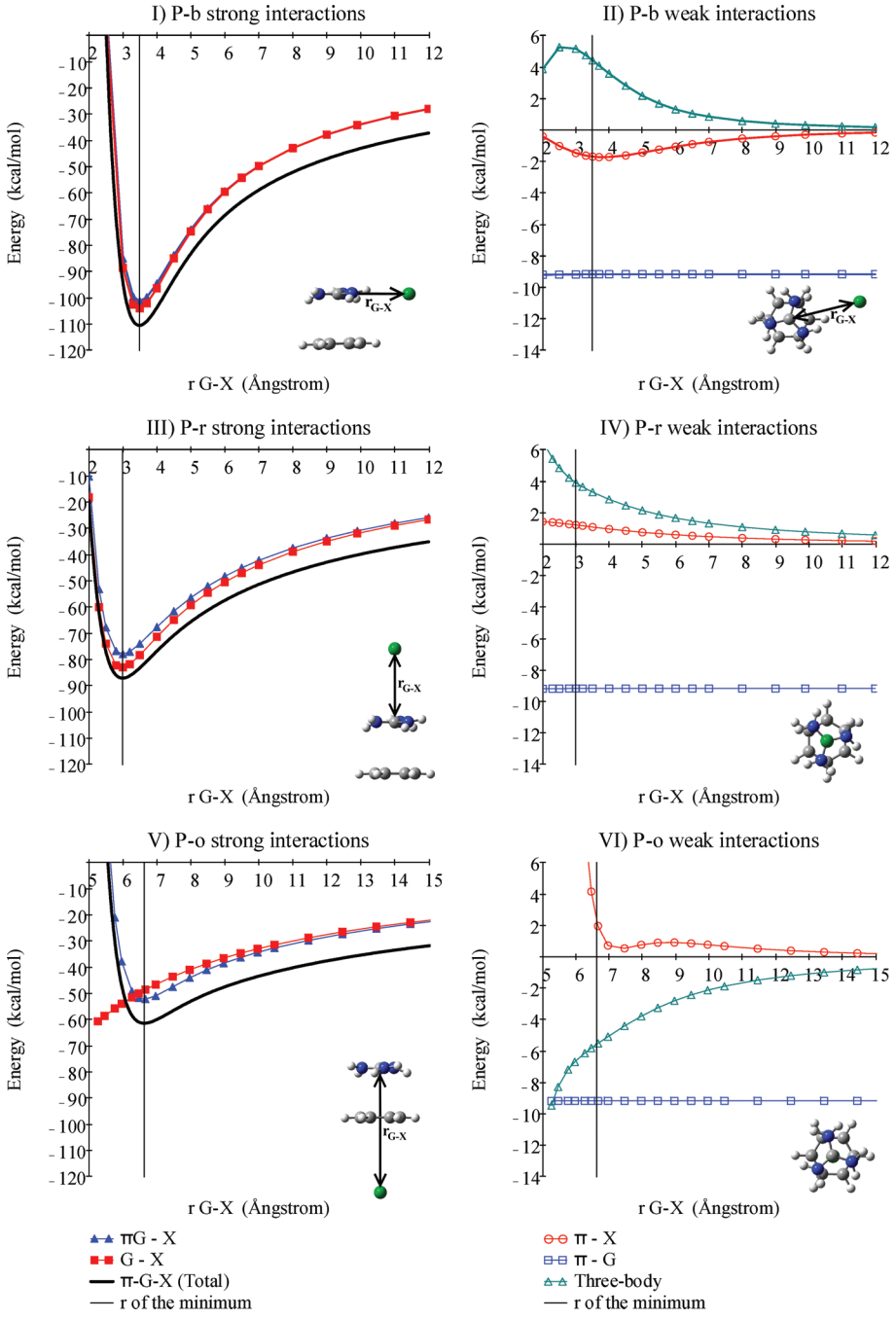

Figure 3. Total and pair interactions of the benzene−guanidinium−chloride system, calculated at the MP2/aug-cc-pVDZ level, when the anion (X = Cl^-) approaches the **P** complex following the three directions indicated.

to the H atom than in the **T-r** trajectory. When the guanidinium cation is displaced above one C−H bond of benzene and the anion approaches parallel to this bond (**D-b** scan), X comes close to the H atom of benzene but does not cross over it, and the anion−π dependence does not show the minimum until the distance between chloride and the guanidinium cation is as short as 2.5 Å. All the rest of the scans present a repulsive anion−π interaction because the anion is moving by trajectories that avoid the direct interaction with the hydrogen atoms of benzene (**P-r**, **D-r**, and **T-b**) or that even directly face the benzene's π cloud (all the **o** directions) that concentrates negative charge.

The shape of the anion−π interaction in the **P-o**, **D-o**, and **T-o** scans is more complex: rather than being monotonically repulsive, these three plots present a minimum and a maximum. This behavior, surprising at first glance, was carefully studied by Coletti and Re in their high-level theoretical study of benzene−halide adducts.[70] As expected, when $E_{\pi-X}$ is represented as a function of the benzene−chloride distance (r_{B-X} instead of r_{G-X}), the three curves are coincident, as can be seen in the inset of Figure 4. This last representation reproduces the position of the minimum (r_{B-X} = 3.81 Å) obtained at the same level of theory by Coletti and Re for the anion−π interaction in the benzene−chloride complex.

dx.doi.org/10.1021/jp302271y | J. Phys. Chem. B 2012, 116, 5860−5871

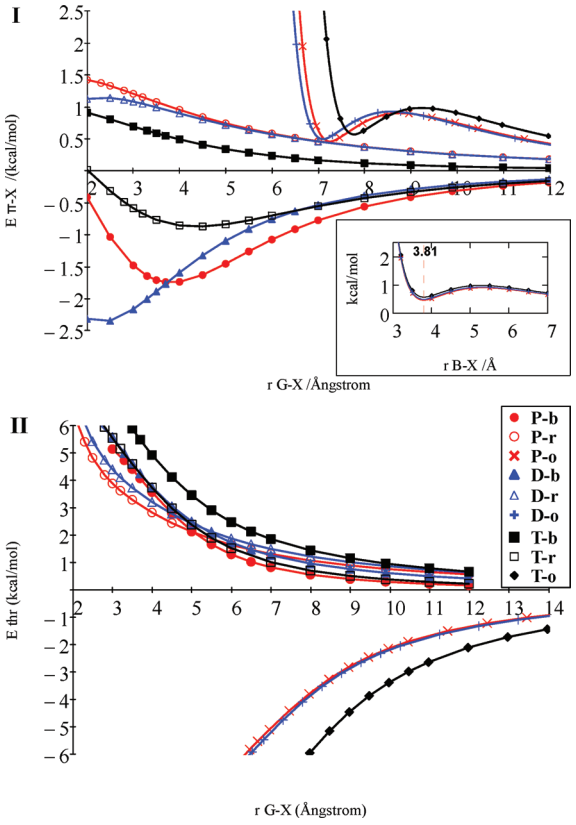

Figure 4. Anion–π ($E_{\pi\text{-X}}$, plot I) and three-body (E_{thr}, plot II) interactions calculated at the MP2/aug-cc-pVDZ level as functions of the guanidinium–chloride distances for the nine BGX scans with X = chloride. The inset in plot I shows the results of $E_{\pi-\text{X}}$ in the o direction as functions of the benzene–chloride distance.

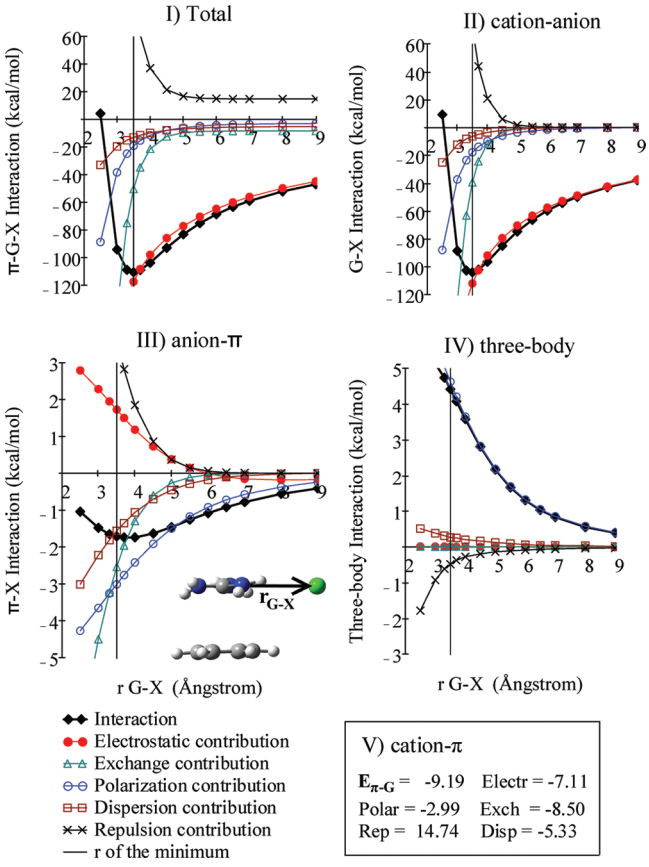

Figure 5. LMO-EDA contributions to the interaction energy for the **P-b** scan at the MP2/aug-cc-pVDZ level at different guanidinium–chloride distances. In the lower-right panel (V), the values, in kcal/mol, for the benzene–guanidinium interaction and its contributions are shown (as the geometry of the BG complex is kept constant in all the points of the scan, these values do not change with $r_{\text{G-X}}$).

The nonadditive term for the nine BGX scans with X = Cl^- analyzed is shown in Figure 4II as a function of the guanidinium–chloride distance. As noted by Kim et al.[43] the three-body interaction is cooperative when the anion and the cation are in opposite sides of the benzene plane: the three **o** trajectories. The most favorable case corresponds to the **T-o** scan because of the bigger polarizing effect of the guanidinium cation when it is perpendicular to the benzene molecule. On the other hand, the values for the scans **P-o** and **D-o** are less negative and very similar, indicating a small influence in the three-body interaction of the displacement of the guanidinium cation from the center of benzene to above one of its C–H bonds when B and G are parallel. In all the other six trajectories studied here, the anion and the cation are in the same side of the benzene molecule, favoring the ion pairing. The cation–anion attraction is always stronger in these trajectories than in the **o** directions, but the **P-b**, **P-r**, **D-b**, **D-r**, **T-b**, and **T-r** scans all exhibit an anticooperative three-body interaction.

3.2.4. Contributions to the Interactions. For obtaining a better understanding of the nature of the different interactions present in the systems studied, the LMO-EDA was applied.[61] Figure 5 shows the results of this analysis for some of the interactions present when a chloride anion moves by the **b** direction toward a benzene–guanidinium complex with **P** geometry (**P-b** scan). At G–X distances larger than approximately 5 Å, exchange, polarization, dispersion, and repulsion contributions to the total interaction (Figure 5I) stabilize in the values corresponding to the BG complex. Of course, the BG–X distance at which contributions different from the electrostatic become constant depends on the geometry of the cation–π complex (**P**, **D**, **T**). Beyond this distance, the main contribution to the total interaction is the electrostatic contribution, and, comparing with Figure 5II, it can be observed that the guanidinium–chloride attraction is mainly (but not solely) responsible for it, in agreement with the expected behavior.

In all the extent of G–X distances explored in the scans (from 2 to 9 Å), the electrostatic as well as the polarization contribution is of great importance in the benzene–chloride interaction (Figure 5III), even when the magnitude of the latter is more than 1 order lower in comparison with the interactions between oppositely charged fragments. As expected, electrostatic and exchange contributions are additive (Figure 5IV), whereas repulsion and dispersion deviate a little from the additivity and almost cancel each other so the nonadditive term has its origin mainly in the polarization. Both cation–π polarization and anion–π polarization contributions are proportionally the most important (Figure 5, plot III and values in the inset V).

If the values of the total interaction or any of its contributions in a binary cation–π complex are subtracted from the values of the total interaction or the same contribution in the corresponding ternary cation–π–anion complex:

$$\Delta E_{\text{Total}} = E_{\text{Total,ternary}} - E_{\text{Total,binary}} \quad (4)$$

dx.doi.org/10.1021/jp302271y | J. Phys. Chem. B 2012, 116, 5860–5871

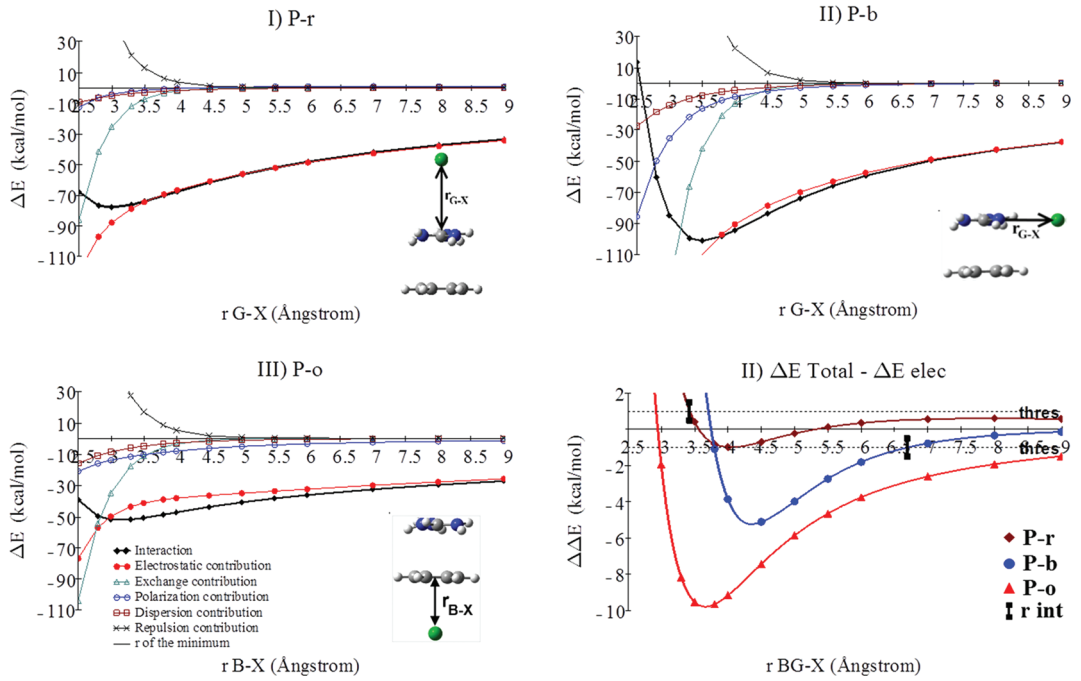

Figure 6. Differences between the total interaction and its contributions in the ternary complex (BGC) with respect to the total interaction and its contribution in the binary (BG) complex for the **P-r**, **P-b**, and **P-o** scans (see text). Plot IV represents the difference ΔE_{Total} and $\Delta E_{\text{electrostatic}}$ of plots I, II, and III. The distance at which the nonelectrostatic contribution of chloride anion exceeds a threshold of ±1 kcal/mol is represented as "r int". For the **P-o** scan, r_{int} is longer than 9 Å.

$$\Delta E_{\text{elec}} = E_{\text{elec,ternary}} - E_{\text{elec,binary}} \quad (5)$$

(and so on), the distance from which the influence of the anion becomes important is highlighted, as can be seen in Figure 6. This kind of representation allows comparing systems of different nature. The behavior observed in Figure 6 for the **P-r** scan is characteristic for all the scans where the anion's approaching direction is **r**: at a BG−X distance approximately half an angstrom larger than the minimum of the corresponding $E_{\pi-\text{G-X}}$ interaction, the curves for the total interaction and the one for its electrostatic contribution are coincident. That is because in this direction, the only interaction that remains at large distances is the electrostatic cation−anion attraction once all other effects of X disappear around 3.5−4.5 Å. On the other hand, Figure 6 shows the characteristic pattern observed when the anion and the cation occupy opposite sides of the benzene plane (all the **o** scans). In these cases, the polarization, mainly due to its anion−π component, propagates over distances longer than in the other X-approaching directions and significantly contributes to the interaction up to BG−X distances longer than 9 Å. These findings are in accordance with the results shown in Figure 4, where for the geometries in which the anion is more distant, the nonadditive term in all the **b** and **r** directions is less than 1 kcal/mol, while the three-body interaction is more than double for the three **o** scans. Finally, the situation shown in Figure 6II is common to all the scans by the **b** direction, where the anion comes directly facing the hydrogen atoms of the guanidinium cation. The difference between the total interaction and its electrostatic contribution is not as pronounced as in the **o** scan,s but it can be still appreciated at 2−3 Å beyond the minimum of the $E_{\pi-\text{G-X}}$ curve. As can be seen in Figure 6II, by the **b** direction, the polarization makes an important contribution up to BG−X distances of about 5.5 − 6.5 Å, and this is because when the anions are in this trajectory, not only is the G−π polarization important (like in the **o** scans), but the G−X polarization is important too.

Besides allowing the classification of the different situations found, the analysis presented before is also useful for obtaining a numerical estimation of the distance at which an anion begins to modulate the cation−π interaction, adding its influence to the long-range electrostatic attraction. Consider the quantity $\Delta\Delta E$, which describes the impact of the anion in the ternary complex on all contributions other than the electrostatic one:

$$\Delta\Delta E = \Delta E_{\text{Total}} - \Delta E_{\text{elec}} \quad (6)$$

In plot IV of Figure 6, the differences $\Delta\Delta E$ for the **P** scans with the chloride anion approaching by the three directions studied are represented. The BG−X distance where the nonelectrostatic effect of the anion over the cation−π interaction exceeds a selected threshold (an arbitrary value of ±1 kcal/mol had been chosen) is defined as "r_{int}". In Figure 6IV, the values of r_{int} for the **P-r** and **P-b** scans (3.68 Å and 6.43 Å, respectively) are represented. For **P-o**, r_{int} > 9 Å, and, consequently, the values of r_{int} are ordered in accordance with the analysis made before.

3.3. Influence of the Anion Nature. As a final step toward understanding the anion effect on the cation−π interactions, two other anions (bromide and nitrate) were used in this study. With Br^-, the geometric configurations examined are the same as those already presented with Cl^-. In the case of nitrate, for all the **b** and **r** scans, the plane of NO_3^- was set to be parallel to the plane of the guanidinium cation, while for those by the **o** approaching direction, NO_3^- is parallel to benzene. This is caused by the fact that when this anion approaches the cation−π complex by the **b** direction, the equilibrium distance between NO_3^- and the BG complexes is larger than when it moves by the other paths (see structures in Figure 9). The M062X/6-31+G* level of calculation is used throughout this

dx.doi.org/10.1021/jp302271y | J. Phys. Chem. B 2012, 116, 5860−5871

section due to the excellent performance observed when comparing the results for Cl^- with the MP2 ones (see Table 1 and Figures S1 to S3 in the Supporting Information).

Table 5 shows the values of the BG−X distance and the $E_{\pi-G-X}$ values for the minima of the total interaction. It is observed that in each direction the interaction is stronger (more negative) for the anion that can approximate more to the cation−π complex: the distance of the most favorable total interaction follows the sequence $Cl^- < Br^- < NO_3^-$ in the **b** direction and $NO_3^- < Cl^- < Br^-$ in all the other cases; the $E_{\pi-G-X}$ values in the minima follow the same trend (including the sign) with the only exception being for the **T-b** scans, where the $E_{\pi-G-X}$ values for NO_3^- and Br^- are inverted, though by less than 0.7 kcal/mol.

Table 5. Interaction Energy ($E_{\pi-G-X}$ in kcal/mol) and Guanidinium−Anion Distance (in Å) for the Minima in the BGX Scans Studied at the M062X/6-31+G* Level[a]

	Cl^-		Br^-		NO_3^-	
X	$E_{\pi-G-X}$	r	$E_{\pi-G-X}$	r	$E_{\pi-G-X}$	r
P-b	−111.60	3.50	−107.63	3.67	−105.96	4.03
D-b	−114.51	3.49	−110.36	3.66	−109.76	4.03
T-b	−113.80	3.50	−109.57	3.67	−110.23	4.02
P-r	−86.81	2.98	−84.61	3.15	−90.54	2.73
D-r	−89.87	2.98	−87.63	3.15	−91.99	2.73
T-r	−94.87	2.97	−92.85	3.13	−97.37	2.72
P-o	−60.81	6.42	−59.80	6.58	−61.90	6.33
		3.07[b]		*3.23*[b]		*2.98*[b]
D-o	−63.39	6.47	−62.27	6.64	−64.87	6.27
		3.17[b]		*3.34*[b]		*2.97*[b]
T-o	−66.85	7.13	−65.62	7.28	−67.97	6.92
		3.15[b]		*3.31*[b]		*2.94*[b]

[a]The BG geometries were kept at the M062X/6-31+G* optimization. [b]Distances between the anion and the centroid of the benzene ring.

The largest differences between the anions studied are observed in the electrostatically controlled E_{G-X}. Figure 7 shows the variation of this interaction for the nine **D** scans, as a function of the cation−anion distance. It is observed that, at large r_{G-X} values, the curves tend asymptotically to a value that corresponds to $E_{\pi-G}$ in the binary complex **D**. At short distances, the curves are grouped depending on the approaching direction of X to the cation−π complex. As seen with chloride, by the **o** direction, the curves show no minimum due to the presence of benzene between the anion and cation, which does not allow for bringing X to the necessary distance. This is not a problem in the **b** and **r** scans, and their minima (r_{G-X} and E_{G-X} values) are clearly influenced by the nature of the anion. By the **r** direction, the nitrate anion can approach the guanidinium cation more than the other anions, and bromide the least, so the strength of the interaction (absolute value of E_{G-X}) follows the sequence $NO_3^- > Cl^- > Br^-$. Moving by the **b** direction, the anions interact directly with the hydrogen atoms of the guanidinium cation that concentrates the positive charge. In this way, the G−X interaction for the **D-b-B** scans (B = Br^-) is about 20 kcal/mol more intense than that for the **D-r-B** scans. By the **b** direction, with the nitrate and guanidinium structures in the same plane, the equilibrium distance for nitrate complex is the largest among the anions studied, so the minimum of E_{G-X} in **D-b-N** (N = NO_3^-) is situated farther than that for **D-b-B**. The results for the approaching of the three anions to **P** and **T** complexes are quite similar to these analyzed here for **D** complexes.

The representation of $E_{\pi-X}$ as a function of the distance between the **P** complex and the different anions (Figure 8I) shows no qualitative differences in comparison with the analyzed scans with X = chloride. Br^- and Cl^- behave in a quite similar fashion, and only NO_3^- presents an anion−π

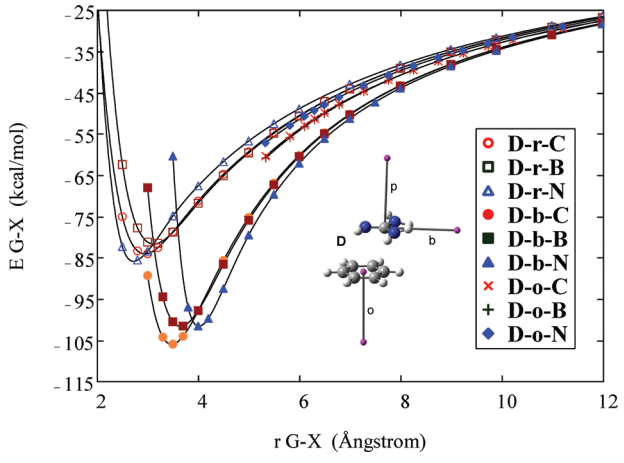

Figure 7. Changes in the cation−anion interaction at the M062X/6-31+G* level as chloride (C), bromide (B), and nitrate (N) approach the **D** complex by the three directions studied.

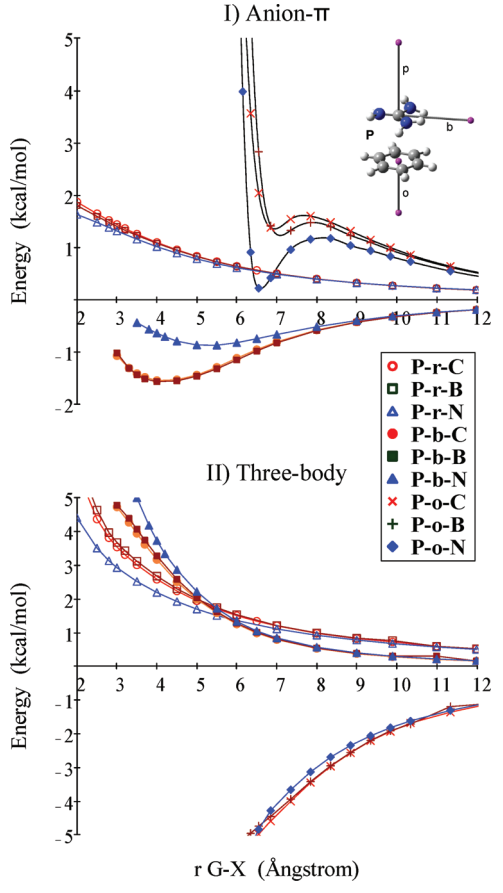

Figure 8. Representation of the interactions $E_{\pi-X}$ and E_{thr} calculated at the M062X/6-31+G* level while chloride (C), bromide (B), and nitrate (N) anions approach the **P** complex by the three studied directions.

dx.doi.org/10.1021/jp302271y | J. Phys. Chem. B 2012, 116, 5860−5871

interaction that is less attractive in **P-b** scans and less repulsive in **P-o** scans, but in all cases the differences are about 1 kcal/mol or smaller. In the **P-r** scans, the three anions show almost the same behavior in all the intervals of BG−X distances examined. The plot of the nonadditive term (Figure 8II) for the same set of scans shows that E_{thr} presents almost identical values when any of the three anions approaches the **P** complex by a particular direction. Only at short BG−X distances is the distinctive nature of the anions revealed, and, again, only NO_3^- slightly deviates from the behavior of Cl^- and Br^-; **P-b-N** is a little more anticooperative than **P-b-C** (C = Cl^-) and **P-b-B**, while **P-r-N** is a little less anticooperative than **P-r-C** and **P-r-B**. For the **o** scans, the nonadditive term is cooperative for the three anions studied, and the values of E_{thr} are almost the same for the **P-o-C**, **P-o-B**, and **P-o-N** scans. The results for the approach of Br^- and NO_3^- to the **D** and **T** complexes (not presented here; see Figures S6 and S7 in the Supporting Information) very much resemble this situation.

Following the pattern already found for the pair interactions, the nature of the anion does not have an outstanding influence in the results of the EDA, and the previous discussion for the scans with chloride is fairly applicable to the scans with bromide and nitrate. The contributions to the total interaction for the **D-b-N**, **D-r-N**, and **D-o-N** scans are presented in Figure 9. The influence of the anion disappears at distances about 2 Å longer than the minimum because the dispersion and polarization contributions quickly become zero. By the **r** direction, the electrostatic contribution is more than 20 kcal/mol weaker than in the **b** scan because the anion−cation configuration is less favorable. By this direction, the nitrate anion can approximate closely to guanidinium, and the BG−NO_3^- distance for the minimum is the smallest among this set of scans. The polarization in **D-r-N** is even less intense than in **D-b-N**, and the influence of the anion vanishes at distances as short as 0.5 Å longer than the minimum. Finally, when nitrate approaches the benzene−guanidinium complex by the opposite side of the benzene molecule (scan **D-o-N**), the electrostatic contribution is even less intense, and (the most outstanding feature of this path) the polarization contribution propagates to very long distances. In this way, by the **o** direction, the influence of the anion is the largest in comparison with the other anion-approaching directions analyzed.

Apart from the anisotropy propitiated by nitrate structure, which pushes out the position of the minimum when the NO_3^- faces the guanidinium cation in the same plane, all the other characteristics of the BGN scans are similar to the analyzed BGC scans and are also applicable to the systems with bromide anion.

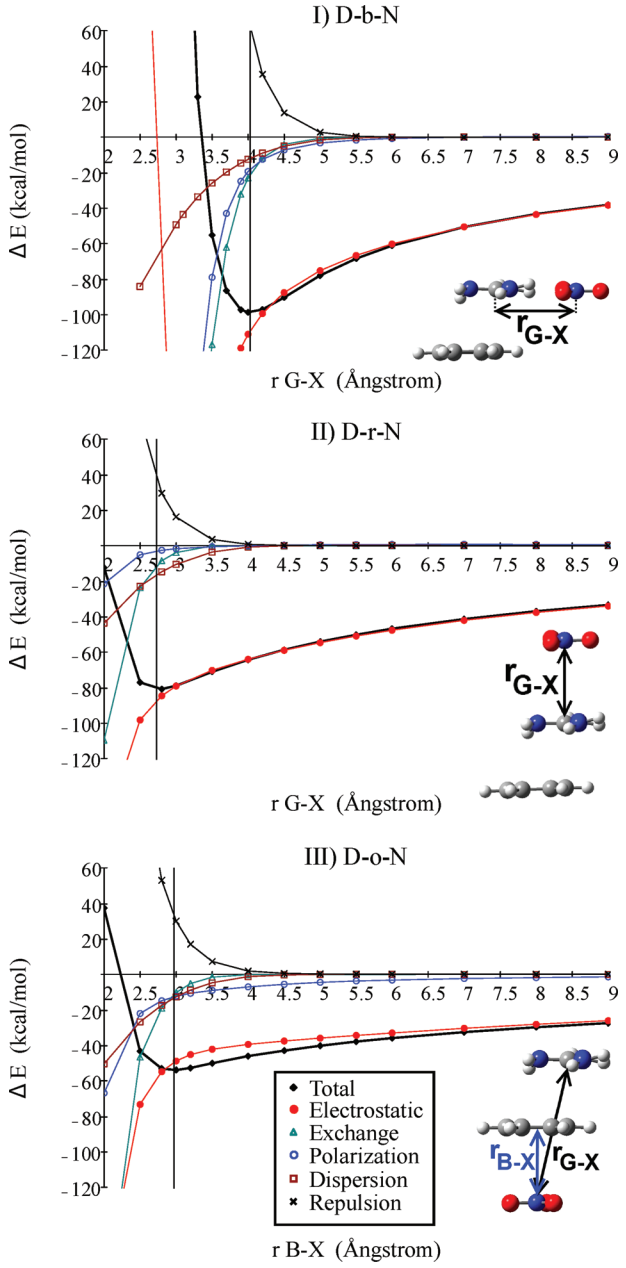

Figure 9. LMO-EDA contributions to the total interaction for the approach of nitrate to the **D** complex by the three directions studied as obtained at the M062X/6-31+G* level. Note that the distances between the cation−π complex and the nitrate anion are expressed as "r_{G-X}" for **D-b-N** and **D-r-N** but as "r_{B-X}" for **D-o-N**.

4. CONCLUSIONS

The characteristics of the interaction in ternary complexes formed by benzene, guanidinium cation, and one anion have been computationally studied employing ab initio and DFT methods. Four minima have been found, most of which correspond to parallel arrangements of guanidinium cation over the benzene unit. All these complexes present the cation and the anion on the same side of the π system, indicating the importance of ion-pairing in the cation−π−anion interaction. Test calculations show that both MP2/aug-cc-pVDZ and M062X/6-31+G* provide results in reasonable agreement with the CCSD(T)/aug-cc-pVDZ level of calculation.

The modulating effect of an anion over the cation−π interaction was systematically studied approaching chloride, bromide, and nitrate anions to benzene−guanidinium complexes using three benzene−guanidinium orientations and, in each case, three approaching directions for the anions. For every BGX arrangement, all pair interactions were calculated, and LMO-EDA was applied for the evaluation of the electrostatic, exchange, repulsion, polarization, and dispersion contributions to the total and pair interactions.

The results confirm that, besides the cation−anion attraction, the effect of X over the B−G interaction is mainly due to the polarization (anion−π and cation−anion) contributions. When the cation and anion are on the same side of the π system, the three-body interaction is anticooperative, and the effect of the anion disappears at short to medium BG−X distances. On the contrary, when the anion and the cation are on opposite sides

dx.doi.org/10.1021/jp302271y | J. Phys. Chem. B 2012, 116, 5860−5871

of the π system, the three-body interaction is cooperative, and the influence of the anion propagates at longer BG−X distances. The main reason for this is the anion−π polarization that extends up to distances longer than 9 Å.

Also, this study shows that the size and geometry of the nitrate ion make no major differences compared with the other anions analyzed. The analysis applied in this work has proven to be a promising tool for the investigation of the influence of anions over the cation−π interaction. The values presented in this work correspond to anion effects on cation−π contacts in the gas phase, so they would represent the behavior of systems where the cation−π contact is buried in a hydrophobic region. Work is in progress for assessing solvent effects in this kind of system.

■ ASSOCIATED CONTENT

Supporting Information

Plots of the total interaction and its pair and three-body components calculated at the MP2/aug-cc-pVDZ level for the T-b, T-r, T-o, D-b, D-r and D-o scans (all with X = Cl^-). Plots of the total, anion−π, and three-body interactions for the P-b, P-r, P-o, T-b, T-r, T-o, D-b, D-r and D-o (all with X = Cl^-) computed at the MP2/aug-cc-pVDZ and M062X/6-31+G* levels of calculation. Plots of the anion-π and three-body interactions calculated at the M062X/6-31+G* level for the scans in which the anions Cl^-, Br^- and NO_3^- approach to the benzene-guanidinium complex by the nine directions explored in this work. Comparison between SAPT(DFT) and LMO-EDA for the ternary minima. This material is available free of charge via the Internet at: http://pubs.acs.org.

■ AUTHOR INFORMATION

Corresponding Author

*E-mail: caba.lago@usc.es.

Notes

The authors declare no competing financial interest.

■ ACKNOWLEDGMENTS

The authors acknowledge the financial support from the Ministerio de Ciencia e Innovación and the ERDF 2007-2013 (Grant No. CTQ2009-12524). We also thank the Centro de Supercomputación de Galicia (CESGA) for the use of their computers.

■ REFERENCES

(1) Meyer, E. A.; Castellano, R. K.; Diederich, F. *Angew. Chem., Int. Ed.* **2003**, *42*, 4120−4120.
(2) Hobza, P.; Zaradnik, R. *Intermolecular Complexes: The Role of van der Waals Systems in Physical Chemistry and the Biodisciplines*; Elsevier: Amsterdam, 1988.
(3) Riley, K. E.; Hobza, P. *Wiley Interdisciplinary Reviews: Computational Molecular Science* **2011**, *1*, 3−17.
(4) Waters, M. L. *Pept. Sci.* **2004**, *76*, 435−445.
(5) Ma, J. C.; Dougherty, D. A. *Chem. Rev.* **1997**, *97*, 1303−1324.
(6) Dougherty, D. A. *J. Nutr.* **2007**, *137*, 1504S−1508S.
(7) Gallivan, J. P.; Dougherty, D. A. *Proc. Natl. Acad. Sci. U.S.A.* **1999**, *96*, 9459−9464.
(8) Lehn, J.-M. *Supramolecular Chemistry*; VCH: Weinheim, Germany, 1995.
(9) Schneider, H.-J.; Yatsimirsky, A. *Principles and Methods in Supramolecular Chemistry*; Wiley: Chichester, U.K., 2000.
(10) Shepodd, T. J.; Petti, M. A.; Dougherty, D. A. *J. Am. Chem. Soc.* **1986**, *108*, 6085−6087.
(11) Shepodd, T. J.; Petti, M. A.; Dougherty, D. A. *J. Am. Chem. Soc.* **1988**, *110*, 1983−1985.
(12) Petti, M. A.; Shepodd, T. J.; Barrans, R. E.; Dougherty, D. A. *J. Am. Chem. Soc.* **1988**, *110*, 6825−6840.
(13) Roelens, S.; Torriti, R. *J. Am. Chem. Soc.* **1998**, *120*, 12443−12452.
(14) Bartoli, S.; Roelens, S. *J. Am. Chem. Soc.* **1999**, *121*, 11908−11909.
(15) Bartoli, S.; Roelens, S. *J. Am. Chem. Soc.* **2002**, *124*, 8307−8315.
(16) Liu, T.; Gu, J.; Tan, X.-J.; Zhu, W.-L.; Luo, X.-M.; Jiang, H.-L.; Ji, R.-Y.; Chen, K.-X.; Silman, I.; Sussman, J. L. *J. Phys. Chem. A* **2001**, *105*, 5431−5437.
(17) Liu, T.; Gu, J.; Tan, X.-J.; Zhu, W.-L.; Luo, X.-M.; Jiang, H.-L.; Ji, R.-Y.; Chen, K.-X.; Silman, I.; Sussman, J. L. *J. Phys. Chem. A* **2001**, *106*, 157−164.
(18) Cheng, Y.-H.; Liu, L.; Fu, Y.; Chen, R.; Li, X.-S.; Guo, Q.-X. *J. Phys. Chem. A* **2002**, *106*, 11215−11220.
(19) Kim, D.; Hu, S.; Tarakeshwar, P.; Kim, K. S.; Lisy, J. M. *J. Phys. Chem. A* **2003**, *107*, 1228−1238.
(20) Soteras, I.; Orozco, M.; Luque, F. J. *Phys. Chem. Chem. Phys.* **2008**, *10*, 2616−2624.
(21) Tsuzuki, S. Interactions with Aromatic Rings. Intermolecular Forces and Clusters I. In *Structure & Bonding*; Springer: Berlin/Heidelberg, 2005; Vol. *115*.
(22) Carrazana-García, J. A.; Rodríguez-Otero, J. s.; Cabaleiro-Lago, E. M. *J. Phys. Chem. B* **2011**, *115*, 2774−2782.
(23) Frontera, A.; Quiñonero, D.; Deyá, P. M. *Wiley Interdisciplinary Reviews: Computational Molecular Science* **2011**, *1*, 440−459.
(24) Quiñonero, D.; Garau, C.; Rotger, C.; Frontera, A.; Ballester, P.; Costa, A.; Deyá, P. M. *Angew. Chem., Int. Ed.* **2002**, *41*, 3389−3392.
(25) Schottel, B. L.; Chifotides, H. T.; Dunbar, K. R. *Chem. Soc. Rev.* **2008**, *37*, 68−83.
(26) Berryman, O. B.; Johnson, D. W. *Chem. Commun. (Cambridge, U. K.)* **2009**, 3143−3153.
(27) Albertí, M.; Aguilar, A.; Lucas, J. M.; Pirani, F.; Coletti, C.; Re, N. *J. Phys. Chem. A* **2009**, *113*, 14606−14614.
(28) Garcia-Raso, A.; Albertí, F. M.; Fiol, J. J.; Lagos, Y.; Torres, M.; Molins, E.; Mata, I.; Estarellas, C.; Frontera, A.; Quiñonero, D.; et al. *Eur. J. Org. Chem.* **2010**, *2001*, 5171−5180.
(29) Ballester, P. *Anions and π-Aromatic Systems. Do They Interact Attractively?* Springer: Berlin/Heidelberg, 2008; Vol. *129*.
(30) Kim, D.; Tarakeshwar, P.; Kim, K. S. *J. Phys. Chem. A* **2004**, *108*, 1250−1258.
(31) Berry, B. W.; Elvekrog, M. M.; Tommos, C. *J. Am. Chem. Soc.* **2007**, *129*, 5308−5309.
(32) Adamo, C.; Berthier, G.; Savinelli, R. *Theor. Chem. Acc.* **2004**, *111*, 176−181.
(33) Singh, N. J.; Min, S. K.; Kim, D. Y.; Kim, K. S. *J. Chem. Theor. Comput* **2009**, *5*, 515−529.
(34) Xu, Y.; Shen, J.; Zhu, W.; Luo, X.; Chen, K.; Jiang, H. *J. Phys. Chem. B* **2005**, *109*, 5945−5949.
(35) Reddy, A. S.; Zipse, H.; Sastry, G. N. *J. Phys. Chem. B* **2007**, *111*, 11546−11553.
(36) Cabaleiro-Lago, E. M.; Rodríguez-Otero, J.; Peña-gallego, A. *J. Chem. Phys.* **2011**, *135*, 214301−9.
(37) Vijay, D.; Zipse, H.; Sastry, G. N. *J. Phys. Chem. B* **2008**, *112*, 8863−8867.
(38) Rao, J. S.; Zipse, H.; Sastry, G. N. *J. Phys. Chem. B* **2009**, *113*, 7225−7236.
(39) Atwood, J. L.; Szumna, A. *J. Am. Chem. Soc.* **2002**, *124*, 10646−10647.
(40) Atwood, J. L.; Szumna, A. *Chem. Commun.* **2003**, 940−941.
(41) Izatt, R. M.; Pawlak, K.; Bradshaw, J. S.; Bruening, R. L. *Chem. Rev.* **1995**, *95*, 2529−2586.
(42) Ngola, S. M.; Kearney, P. C.; Mecozzi, S.; Russell, K.; Dougherty, D. A. *J. Am. Chem. Soc.* **1999**, *121*, 1192−1201.
(43) Kim, D.; Lee, E. C.; Kim, K. S.; Tarakeshwar, P. *J. Phys. Chem. A* **2007**, *111*, 7980−7986.

(44) Albertí, M.; Aguilar, A.; Lucas, J. M.; Pirani, F. *J. Phys. Chem. A* **2010**, *114*, 11964−11970.
(45) Albertí, M.; Aguilar, A.; Pirani, F. *J. Phys. Chem. A* **2009**, *113*, 14741−14748.
(46) Frontera, A.; Quiñonero, D.; Costa, A.; Ballester, P.; Deyá, P. M. *New J. Chem.* **2007**, *31*, 556−560.
(47) Duffy, E. M.; Kowalczyk, P. J.; Jorgensen, W. L. *J. Am. Chem. Soc.* **1993**, *115*, 9271−9275.
(48) Mason, P. E.; Neilson, G. W.; Dempsey, C. E.; Barnes, A. C.; Cruickshank, J. M. *Proc. Natl. Acad. Sci. U. S. A.* **2003**, *100*, 4557−4561.
(49) Mason, P. E.; Neilson, G. W.; Enderby, J. E.; Saboungi, M.-L.; Dempsey, C. E.; MacKerell, A. D., Jr.; Brady, J. W. *J. Am. Chem. Soc.* **2004**, *126*, 11462−11470.
(50) Vondrasek, J.; Mason, P. E.; Heyda, J.; Collins, K. D.; Jungwirth, P. *J. Phys. Chem. B* **2009**, *113*, 9041−9045.
(51) Blanco, F.; Kelly, B.; Alkorta, I.; Rozas, I.; Elguero, J. *Chem. Phys. Lett.* **2011**, *511*, 129−134.
(52) Rozas, I.; Kruger, P. E. *J. Chem. Theor. Comput.* **2005**, *1*, 1055−1062.
(53) Plaquevent, J.-C.; Levillain, J.; Guillen, F. d. r.; Malhiac, C.; Gaumont, A.-C. *Chem. Rev.* **2008**, *108*, 5035−5060.
(54) Greaves, T. L.; Drummond, C. J. *Chem. Rev.* **2007**, *108*, 206−237.
(55) Chałasiński, G.; Szczęśniak, M. M. *Chem. Rev.* **2000**, *100*, 4227−4252.
(56) Boys, S. F.; Bernardi, F. *Mol. Phys.* **1970**, *19*, 553−566.
(57) Frisch, M. J.; Trucks, G. W.; Schlegel, H. B.; Scuseria, G. E.; Robb, M. A.; Cheeseman, J. R.; Scalmani, G.; Barone, V.; Mennucci, B.; Petersson, G. A.et al. Gaussian, Inc.: Wallingford, CT, 2009.
(58) Cabaleiro-Lago, E. M.; Rios, M. A. *J. Chem. Phys.* **2000**, *112*, 2155−2163.
(59) Elrod, M. J.; Saykally, R. J. *Chem. Rev.* **1994**, *94*, 1975−1997.
(60) Vijay, D.; Sastry, G. N. *Chem. Phys. Lett.* **2010**, *485*, 235−242.
(61) Su, P.; Li, H. *J. Chem. Phys.* **2009**, *131*, 014102−15.
(62) Gordon, M. S.; Schmidt, M. W. In *Theory and Applications of Computational Chemistry*; Dykstra, C. E., Frenking, G., Kim, K. S., Scuseria, G. E., Eds.; Elsevier: Amsterdam, 2005.
(63) Schmidt, M. W.; Baldridge, K. K.; Boatz, J. A.; Elbert, S. T.; Gordon, M. S.; Jensen, J. H.; Koseki, S.; Matsunaga, N.; Nguyen, K. A.; Su, S.; et al. *J. Comput. Chem.* **1993**, *14*, 1347−1363.
(64) Kitaura, K.; Morokuma, K. *Int. J. Quantum Chem.* **1976**, *10*, 325−340.
(65) Ziegler, T.; Rauk, A. *Inorg. Chem.* **1979**, *18*, 1755−1759.
(66) Hayes, I. C.; Stone, A. J. *Mol. Phys.* **1984**, *53*, 83−105.
(67) Jeziorski, B.; Moszynski, R.; Szalewicz, K. *Chem. Rev.* **1994**, *94*, 1887−1930.
(68) Misquitta, A. J.; Podeszwa, R.; Jeziorski, B.; Szalewicz, K. *J. Chem. Phys.* **2005**, *123*, 214103−14.
(69) Werner, H.-J.; Knowles, P. J.; Manby, F. R.; Schütz, M.; Celani, P.; Knizia, G.; Korona, T.; Lindh, R.; Mitrushenkov, A.; Rauhut, G.et al. Molpro version 2009.1, a package of ab initio programs, see http://www.molpro.net.
(70) Coletti, C.; Re, N. *J. Phys. Chem. A* **2009**, *113*, 1578−1585.